EMPOWERING YOUR DISCOVERY

Cytek® Northern Lights™ System

Full spectrum flow cytometry empowers your single cell discovery - with fewer hurdles and easy-to-follow workflows. Join leading scientists and researchers at academic and pharmaceutical institutions who are accelerating time to insight with flexible panel design and expanded reagent options.

- **Ease-of-use:** Cytek Assay Settings come with every system, simplifying instrument setup and removing the need to optimize individual detectors.
- **Compatibility with Existing Panels:** Capable of running any assay from your current 1-3 laser system.
- **Enhanced Sensitivity and Resolution:** Easily gate and resolve rare and dim cell populations.

There has never been a better time to join the shift to Full Spectrum Profiling™ (FSP™).

CYTEK®
TRANSCEND THE CONVENTIONAL
cytekbio.com

Received: 8 September 2022 | Revised: 27 October 2022 | Accepted: 28 November 2022

DOI: 10.1002/cyto.a.24708

ORIGINAL ARTICLE

MIFlowCyt

ISAC INTERNATIONAL SOCIETY FOR ADVANCEMENT OF CYTOMETRY

CYTOMETRY Journal of Quantitative Cell Science PART A

iCoreDrop: A robust immune monitoring spectral cytometry assay with six open channels for biomarker flexibility

Holly A. Jensen | **Jeong Kim**

Translational Research, Tumor Microenvironment Thematic Research Center, Bristol Myers Squibb, Redwood City, California, USA

Correspondence
Holly A. Jensen, Bristol Myers Squibb, 700 Bay Road, Redwood City, California, 94063, USA.
Email: haj25@cornell.edu

Abstract

Recent advances in spectral cytometry have extended our ability to monitor immune cell subsets and activation status while simultaneously improving rare population detection. However, technical challenges in reference control selection and autofluorescence extraction serve as barriers to broad application of spectral flow cytometry. Furthermore, the complexity of spectral cytometry panel development limits the adaptation of established assays. Here, we describe the development of a spectral immunophenotyping assay with robust drop-in capability to enable biomarker interrogation flexibility. The immune monitoring core (iCore), which can be used in part or total, captures broad and granular immune subsets across T cells, B cells, NK cells, monocytes, dendritic cells, and granulocytes in peripheral whole blood. Additional user-selected biomarkers can be dropped in (Drop) using channels BV421, Alexa Fluor 488, PE, PE-Cy7, APC, and APC-Cy7. A comprehensive assessment of reagent and panel performance was conducted, including reference control comparison and optimal autofluorescence (AF) extraction on the 5-laser Cytek Aurora system for healthy donor blood. Assay precision and stability analyses revealed robust intra-assay precision, with 95% of 83 distinct population gates having <20% CV. In the presence of additional drop-in markers in two different settings, a T cell module and a myeloid/B cell module, the drop-in channels themselves achieved <20% CV across 12 out of 13 additionally queried population gates. Overall, establishment of optimal unmixing practices will enable widespread adoption of spectral cytometry assays.

KEYWORDS
autofluorescence, Cytek Aurora, drop-in channels, precision, spectral cytometry, reference controls

1 | INTRODUCTION

For biomarker development, cytometry assays offer advantages over other multiplex methodologies due to real-time sample analysis, lower cost, and comparatively rapid data turnaround. However, poor reproducibility for rare populations, reduced resolution after fluorescence spill-over correction, and non-optimized data analysis practices can undermine the benefits of cytometry assays within translational and clinical biomarker strategies. These conventional shortcomings are remitted by the advent of spectral cytometry, which has propelled robust cytometry assay development. The Cytek Aurora, for example, is an advanced spectral cytometer capable of profiling 30–40 biomarkers while simultaneously improving rare population detection.

Typically, immunophenotyping assays rely on a core of commonly employed immune lineage markers or subset thereof [1–6]. Based on an extensive literature review, high-parameter immune monitoring cytometry assays include on-average an additional 6 to 7 biomarkers of interest (Supplemental Figure 1A,B). The largest immune panel designs of 30+ markers include auxiliary modules for activation or immune accessory molecules, B cell lineage maturation, T cell receptors, transcription factors, or cytokines (Supplemental Figure 1C–I). Unfortunately, these designs allow little to no flexibility for custom applications. Despite the multitude of published immunophenotyping assays available, de novo panels continue to be developed.

To address these challenges, we developed a core pan-immune monitoring spectral cytometry assay (iCore) with six open drop-in channels (Drop). For the iCore, we identified the top immune markers employed in 20% or more of 60+ published OMIPs and immunophenotyping panels (Supplemental Figure 1A). These include the marker for total leukocytes (CD45); primary lineage markers for T cells, B cells, NK cells, monocytes, and granulocytes (CD3, CD4, CD8, CD19, CD56, CD14, CD16); lymphoid memory, regulatory, and activation markers (CD45RA, CCR7, CD27, CD28, IgD, CD127, CD25, CD38, CD57, CD161); chemokine receptors (CXCR3, CXCR5, CCR4, CCR6); γδ T cells (TCRγδ); and dendritic cell subsets (HLA-DR, CD11c, CD123). Final selections were adjusted to include broadly co-expressed myeloid markers that can be challenging to incorporate: CD33, CD11b, and CD15 for myeloid-derived suppressor cell (MDSC) identification. The iCore can be used as a stand-alone panel on the Cytek Aurora or other spectral cytometer, with the optional addition of markers on the following six bright and widely available fluorophores: BV421, Alexa Fluor 488 (AF488), PE, PE-Cy7, APC, and APC-Cy7 (Supplemental Figure 1J). The iCoreDrop can also serve as a cost-effective, spectral cytometry substitute for the Standard BioTools (previously Fluidigm) MaxPar Direct Immune Profiling Kit designed for mass cytometry [7].

Highly informative guidelines toward spectral cytometry assay development have been published [8–10], but end-users continue to struggle with proper reference control application and unmixing practices. Here, we show that the final iCoreDrop panel (Figure 1) exhibits robust assay performance on human blood due to thorough reference control interrogation and unmixing optimization. Guidance on single stain control tracking and format, autofluorescence extraction, and gating strategy for the iCore is provided. Two iCoreDrop examples employing added T cell markers (CTLA-4, CD103, PD-1, TIGIT, CCR5, CD95) or myeloid and B cell markers (CD117, CD163, CD141, CD1c, CD86, CD24) demonstrate that the observed repeatability of the iCore is maintained in the presence of additional drop-in biomarkers.

2 | MATERIALS AND METHODS

2.1 | Sample preparation

Healthy donor whole blood was collected through the BMS volunteer collection program in accordance with company guidelines. Peripheral blood was collected in Na-Heparin tubes and processed at 0 h or stored at 4°C until processing at 24 or 48 h. RBC-lysed whole blood processed at 24 h was employed for this work unless otherwise specified. 3 ml whole blood aliquots were lysed using 7 ml 1X BD Pharm Lyse Buffer (BD Biosciences, Franklin Lakes NJ, USA) for 15 min at room temperature (RT). RBC-lysed blood was centrifuged at 300 × g for 5 min and leukocyte pellets were resuspended in another 7 ml 1X BD Pharm Lyse Buffer for 10 min at RT. Twice RBC-lysed blood was centrifuged at 300 × g for 5 min and leukocyte pellets were resuspended in 500 µl of Staining Buffer (BD Biosciences). 30 µl of 6X concentrated blood was used per test.

For PBMC isolation, 10 ml whole blood was diluted 1:1 with Ca^{+2}/Mg^{+2}-free PBS (Corning, Corning NY, USA) and placed above the frit of Accuspin tubes (Millipore Sigma, Burlington MA, USA) containing 15 ml Histopaque (Millipore Sigma) below the frit and centrifuged at 800 × g for 20 min with the brake off. The buffy coat was removed and washed twice with Ca^{+2}/Mg^{+2}-free PBS at 300 × g for 10 min before resuspension in Freezing Media with 90% FBS and 10% DMSO (Thermo Scientific, Waltham MA, USA) followed by storage at −80°C. Cryopreserved PBMC were thawed by quickly heating cryovials in a 37°C water bath and pipetting drop-wise into 9 ml of prewarmed RPMI media (Thermo Scientific) before centrifugation at 300 × g for 5 min and resuspension in Staining Buffer.

2.2 | Flow cytometry staining

Panel staining reagents are detailed in Table 1 (iCore reagents). Reagents for CD4 Cross Stain Index matrix generation are shared in Supplemental Figure 2B. Resuspended leukocytes (6X concentrated RBC-lysed blood) were treated with 1:25 (20 µg/ml) of Human Fc block (BD Biosciences) for 10 min at RT. For optimized staining, we added 0.6 µl per test of TCRγδ PerCP-eF710 for 10 min at RT. Next, we added 2.5 µl each of diluted CCR7 BV711 and CD25 PE-AF700 per test and incubated sample tubes at 37°C for 20 min, followed by incubation with remaining antibody reagents at 4°C for 45 min. We then added 400 µl of Ca^{+2}/Mg^{+2}-free PBS per test and centrifuged at 300 × g for 5 min, followed by resuspension of the pellets in 100 µl of 1:1000 LIVE/DEAD Blue (Thermo Scientific) in Ca^{+2}/Mg^{+2}-free PBS at 4°C for 20 min. After incubation, 400 µl of Staining Buffer was added per test and centrifuged at 300 × g for 5 min followed by resuspension in 200 µl of Ca^{+2}/Mg^{+2}-free PBS before acquisition.

For cell-based single stain reference controls, the equivalent staining procedure above was used. Bead-based reference controls were prepared by incubating 1 µl of antibody reagent at least 2 min at RT with 30 µl of UltraComp beads (Thermo Fisher) or SpectraComp beads (Slingshot Biosciences, Emeryville CA, USA) before resuspension in Ca^{+2}/Mg^{+2}-free PBS. Negative bead backgrounds were captured in separate unstained tubes, as low intensity positive staining was often observed for in-tube negative beads. Reagents captured on both bead formats were brighter than the cell-based controls, and cell-based controls were as bright as multicolor samples. Positive single stain control samples for LIVE/DEAD Blue were established by placing resuspended leukocytes at 60°C for 20 min to kill cells. LIVE/DEAD Blue titration was performed using thawed cryopreserved PBMC. Titrations were performed using 4°C incubation for 45 min only, with some markers being titrated again at optimized staining conditions.

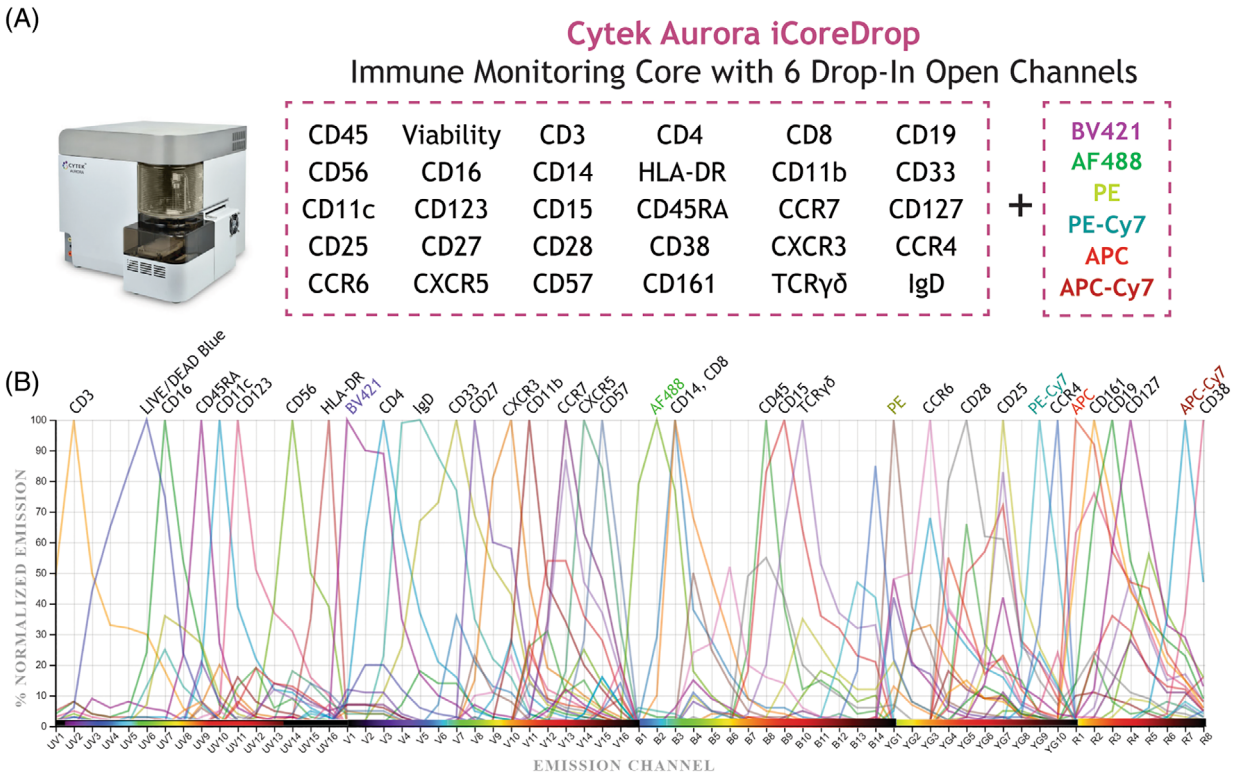

(C)

Drop-In Guide

Drop-In Position	Fluorophore Options	Could Impact or Be Impacted By	Example T cell Module	Example Myeloid/B cell Module
1	**BV421**, SB436*	CD4	CTLA-4	CD117
2	BB515, FITC, **AF488**	CD33, CD14, CD8	CD103	CD163
3	**PE**, cFluor YG584	CD45RA, IgD, CD27, CD14, CD8	PD-1	CD141
4	**PE-Cy7**, PE-Vio770, cFluor BYG781	CD57, TCRγδ, CCR4	TIGIT	CD1c
5	**APC**, cFluor R780	CD123, CD11b, TCRγδ, CD161, CD19	CCR5	CD86
6	**APC-Cy7**, APC-H7, APC-Vio770 APC-Fire 750, APC-eF780	HLA-DR, CD57, CD38	CD95	CD24

FIGURE 1 iCoreDrop concept. The iCore immune biomarkers profiled within the iCoreDrop are listed alongside available drop-in channels (A). The normalized spectral signatures for all iCoreDrop components are shown for reference (B). Equivalent drop-ins for each open channel are listed, along with iCore markers that could impact or be impacted by these channels (C). Fluorophore drop-ins tested in this work are highlighted in bold. Note (*) that Super Bright 436 (SB436) could be used in combination with BV421 with careful panel design. Example drop-in markers explored in this work are shown: a T cell module and a myeloid/B cell module.

2.3 | Instrument performance and Unmixing

All samples were acquired on a 5-laser Cytek Aurora (Cytek Biosciences, Fremont CA, USA) using the Cytek Assay Settings. Instrument performance was monitored daily using QC beads. We calculated the CD4-based Cross Stain Index Matrix (Supplemental Figure 2A) and found our instrument performance to be highly similar to four other recently reported 5-laser Cytek Auroras [8]. We consistently employed tubes for this work to avoid potential flow rate and performance differences between tube and plate mode.

2.4 | Data analysis

Exported .fcs files were gated and analyzed for % population, %CV, and stain index using FCS Express 7 (De Novo Software, Pasadena CA, USA). We developed a gating strategy that contained over 80 gates for the iCore (Figure 3). All %CV values are based on %Frequency of Parent (%FoP) per population. For Cross Stain Index (CSI) matrix calculations, we used CSI calculation tools which are available at https://denovosoftware.com/about-us/partnerships/partnership-cytek/cytekfcsexpress/. For Similarity Index, we pulled values

TABLE 1 iCore reagent information

Marker	Clone	Fluorophore	Vendor	Catalog no.	Stock conc. (μg/ml)	Reagent stability (days)	μl per test	Working dilution	Dilution stability (days)	Staining
CD3	UCHT1	BUV395	BD	563548	200	187	0.31	8X	42	4C, 45 min
Viability	-	Live/Dead BLUE	Thermo	L23105	-	-	0.10	1000X	-	4C, 20 min
CD16	3G8	BUV496	BD	612945	300	261	2.50	-	-	4C, 45 min
CD45RA	HI100	BUV563	BD	612927	50	261	0.31	8X	58	4C, 45 min
CD11c	B-Ly6	BUV615	BD	752531	200	141	0.31	8X	42	4C, 45 min
CD123	6H6	BUV661	BD	751838	200	<48	0.31	8X	<7	4C, 45 min
CD56	NCAM16.2	BUV737	BD	612766	25	384	0.31	8X	21	4C, 45 min
HLA-DR	L203	BUV805	BD	752497	50	231	0.31	8X	42	4C, 45 min
CD4	RPA-T4	Pacific Blue	Biolegend	300524	500	261	0.63	4X	42	4C, 45 min
IgD	IA6-2	BV480	BD	566187	200	193	0.63	4X	58	4C, 45 min
CD33	WM53	BV510	Biolegend	303421	25	231	0.31	8X	42	4C, 45 min
CD27	O323	BV570	Biolegend	302825	25	98	1.25	2X	42	4C, 45 min
CXCR3	G025H7	BV605	Biolegend	353727	150	12	5.00	-	-	4C, 45 min
CD11b	ICRF44	BV650	Biolegend	301335	100	193	2.50	-	-	4C, 45 min
CCR7	G043H7	BV711	Biolegend	353227	100	191	1.25	2X	42	37C, 20 min
CXCR5	J252D4	BV750	Biolegend	356941	100	191	1.25	2X	58	4C, 45 min
CD57	QA17A04	BV786	Biolegend	393329	100	384	0.31	8X	58	4C, 45 min
CD14	63D3	Spark Blue 550	Biolegend	367147	100	193	0.63	4X	42	4C, 45 min
CD8	RPA-T8	AF532	Thermo	58-0088-42	25	384	1.25	2X	13	4C, 45 min
CD45	HI30	PerCP	Biolegend	304025	200	191	1.25	2X	42	4C, 45 min
CD15	W6D3	PerCP-Cy5.5	Biolegend	301921	25	<20	2.50	-	-	4C, 45 min
TCRγδ	B1.1	PerCP-eF710	Thermo	46-9959-42	400	<40	0.63	-	<1	RT, 10 min
CCR6	G034E3	PE-Dazzle 594	Biolegend	353429	50	191	1.25	2X	58	4C, 45 min
CD28	CD28.2	PE-Cy5	Biolegend	302910	100	231	0.31	8X	42	4C, 45 min
CD25	CD25-3G10	PE-AF700	Thermo	MHCD2524	100	161	0.63	4X	<7	37C, 20 min
CCR4	L291H4	PE/Fire 810	Biolegend	359433	100	12	0.31	8X	21	4C, 45 min
CD161	HP-3G10	AF647	Biolegend	339909	180	141	0.63	4X	42	4C, 45 min
CD19	HIB19	Spark NIR 685	Biolegend	302269	100	191	1.25	2X	58	4C, 45 min
CD127	HIL-7R-M21	APC-R700	BD	565185	100	291	1.25	2X	70	4C, 45 min
CD38	HIT2	APC/Fire 810	Biolegend	303549	25	384	0.63	4X	111	4C, 45 min

Note: Table 1 details reagent information for the iCore, including target immune marker, clone, fluorophore, vendor, catalog no., and stock concentration. Additionally, stock reagent stability, μl per test, working dilution factor, dilution stability and staining temperature are detailed for easy reference. A thorough understanding of reagent performance and appropriate reference controls (see Table 2) is crucial to successful application of the multicolor assay.

calculated directly within SpectroFlo v 2.0 software (Cytek Biosciences) during unmixing. Two-tailed student's t-tests were calculated in Excel (Microsoft, Redmond WA, USA). We used Excel, GraphPad Prism 7 (Dotmatics, Boston MA, USA), and Adobe Illustrator (Adobe, San Jose CA, USA) to generate final tables, graphs, and figures.

3 | RESULTS

3.1 | Panel development summary

Based on established guidance for spectral cytometry assay design and development, we assigned fluorophore channels to each marker considering immune marker expression, fluorophore brightness and spillover, and clone availability [8–10]. We also reviewed commonalities between OMIP-069 [1] and other large 30+ color spectral cytometry panels [2–4, 6, 11] which are suggestive of robust marker-fluor assignments. One unique challenge here was maintaining six open channels on bright, widely available fluorophores which could not be used for iCore marker assignment.

Over the course of panel development we eliminated PD-1 from the iCore, and removed fluorophores Pacific Orange and BB515, while taking advantage of newly released APC/Fire 810 and PE/Fire 810 (Supplemental Figure 9). While iterative marker-fluor reassignment was critical to successful panel design, a comprehensive assessment of reagent performance and unmixing conditions was also

required to reduce or eliminate persistent issues. We optimized staining concentration, staining procedure, working dilution stability, reference controls, and autofluorescence extraction, while also using CSI matrices and N × N plots to QC overall panel performance (see below). The final iCore panel design and information are shown in Figure 1 with details provided in Table 1.

3.2 | Reagent performance

To determine the optimal concentration of staining reagents, standard antibody reagent titrations were performed (Table 1, Supplemental Figure 3). Additionally, we utilized the Similarity Index calculated within SpectroFlo software to inform reagent stock stability (Figure 2A) and dilution integrity (Supplemental Figure 4C) over time. We considered a Similarity Index (SI) greater than or equal to 0.999 to represent near identical (stable) spectral profiles, while a SI <0.999 is indictive of burgeoning deviations between spectral profiles. Most antibody reagents are highly stable when handled and stored properly (Figure 2A). Notably, CD3 BUV395 and CD11b BV650 showed changes in spectral profile after 200+ days. Some reagents displayed drops in Similarity Index (CD27 BV570, CD14 Spark Blue 550) which appeared to be technical artifacts and were not correlated to any consistent spectral profile change.

However, BUV661 and PerCP-Cy5.5 were identified as relatively unstable fluorophores. CD123 BUV661 is highly similar initially, then exhibits a spectral degradation effect that alters signal in red off-channels (Supplemental Figure 7A) which then stabilizes. The most strikingly unstable reagent in the iCore is CD15 PerCP-Cy5.5, whose spectral profile is highly variable between comparisons (SIs <0.999) and the reagent lot was exhausted before approaching consistent performance (Figure 2A). Comparison of separate reagent lots was not a goal of this work, but we empirically noted little-to-no significant performance differences between new reagent lots, with the exception of reagents that tended to differ over time (i.e., CD15 PerCP-Cy5.5). In short, it is highly recommended that single stain controls for CD123 BUV661 and CD15 PerCP-Cy5.5 be captured week to week.

For assay precision, dilutions are recommended for antibody reagents requiring less than 2.5 µl per test, and we tracked the integrity of these dilutions over time. Most reagents are stable in Staining Buffer for 21–58 days, but notable exceptions include TCRγδ PerCP-eF710 and CD25 PE-AF700 (Supplemental Figure 4C). CD25 PE-AF700 resolution is reduced when using 5–7-day old dilutions, while TCRγδ PerCP-eF710 staining disappears entirely using dilutions only 24 h old. CD123 BUV661 dilutions can also differ over time due to the reagent's inherent instability described above. Thus, dilutions for CD123 BUV661, TCRγδ PerCP-eF710, and CD25 PE-AF700 should be prepared fresh or avoided.

We performed staining temperature comparisons and found that most immune markers stain similarly at 4 and 37°C (Supplemental Figure 4G). Whereas the performance of most antibodies was not adversely affected by staining temperature, the antibodies specific for TCRγδ, the chemokine receptor CCR7, and the high affinity IL-2 receptor CD25 were sensitive to staining conditions. Like OMIP-069, we found that staining TCRγδ PerCP-eF710 for 10 min at room temperature prior to the remaining antibodies greatly improved detection (Supplemental Figure 4D), and reconfirmed titration results at these conditions. The chemokine receptor CCR7 is known to exhibit rapid cell-surface cycling and was particularly improved upon staining at 37°C (Supplemental Figure 4F). CD25 PE-AF700 also stained better at 37°C (Supplemental Figure 4E). Thus, these two reagents are added during a separate 37°C staining step. Minimal cell death occurs over the extended multi-temperature staining sequence (Supplemental Figure 4H).

Overall, elucidating these intrinsic reagent properties (fluorophore stability, dilution stability, optimal staining) was an important step prior to inspection of single stain reference control formats.

3.3 | Reference controls

Determining the optimal single stain reference controls is a crucial factor to successful unmixing. The recently released SpectraComp beads (Slingshot Biosciences) are designed to simulate cell autofluorescence, and we posited that SpectraComp beads could improve upon conventional compensation beads and/or better corroborate cell-based profiles. To this end, single reagent spectral performances on UltraComp and SpectraComp beads were compared to cells using Similarity Index (Figure 2B). While many bead versus cell spectral profiles were highly similar with SI >0.999, some fluorophores differed such as CD11c BUV615, CXCR3 BV605, CD56 BUV737, CD8 AF532, CD25 AF-PE700, CD38 APC/Fire 810 and more strikingly, CD45 PerCP, CD15 PerCP-Cy5.5, and TCRγδ PerCP-eF710 (Figure 2B). Also, instability in the red channel region of CD123 BUV661 (as described above) can contribute to failed bead versus cell tests.

To understand how different reference control formats impact unmixing, N × N plots of fully stained samples were examined after replacing each single stain with either an UltraComp, SpectraComp, or cell-based reference control. Approximately half of the iCore reagents could be unmixed with either UltraComp, SpectraComp, or cell-based reference controls with no discernable difference, including most BV dyes and all PE tandems (Table 2). Interestingly, this interchangeability holds true for some regents for which bead versus cell-based spectral profiles exhibited lower similarity (CD11c BUV615, CXCR3 BV605, CD8 AF532, CD25 PE-A700).

For the remaining reagents, optimized reference controls typically improved neighboring or spectrally correlated markers, (markers whose assigned fluorophore could be impacted by overlapping local emission maxima, see Supplemental Figure 5B). Notable improvements are detailed in Table 2. In some cases SpectraComp reference controls improved unmixing results despite essentially identical similarity between bead and cell-based spectral profiles. CD45RA BUV563, CD14 Spark Blue 550, and CD19 Spark NIR 685 SpectraComp beads all improved neighboring or correlated markers (Table 2, Supplemental Figure 6). CD16 BUV496 SpectraComp beads improved CD3 BUV395 with negligible reduction in CD33 BV510 resolution,

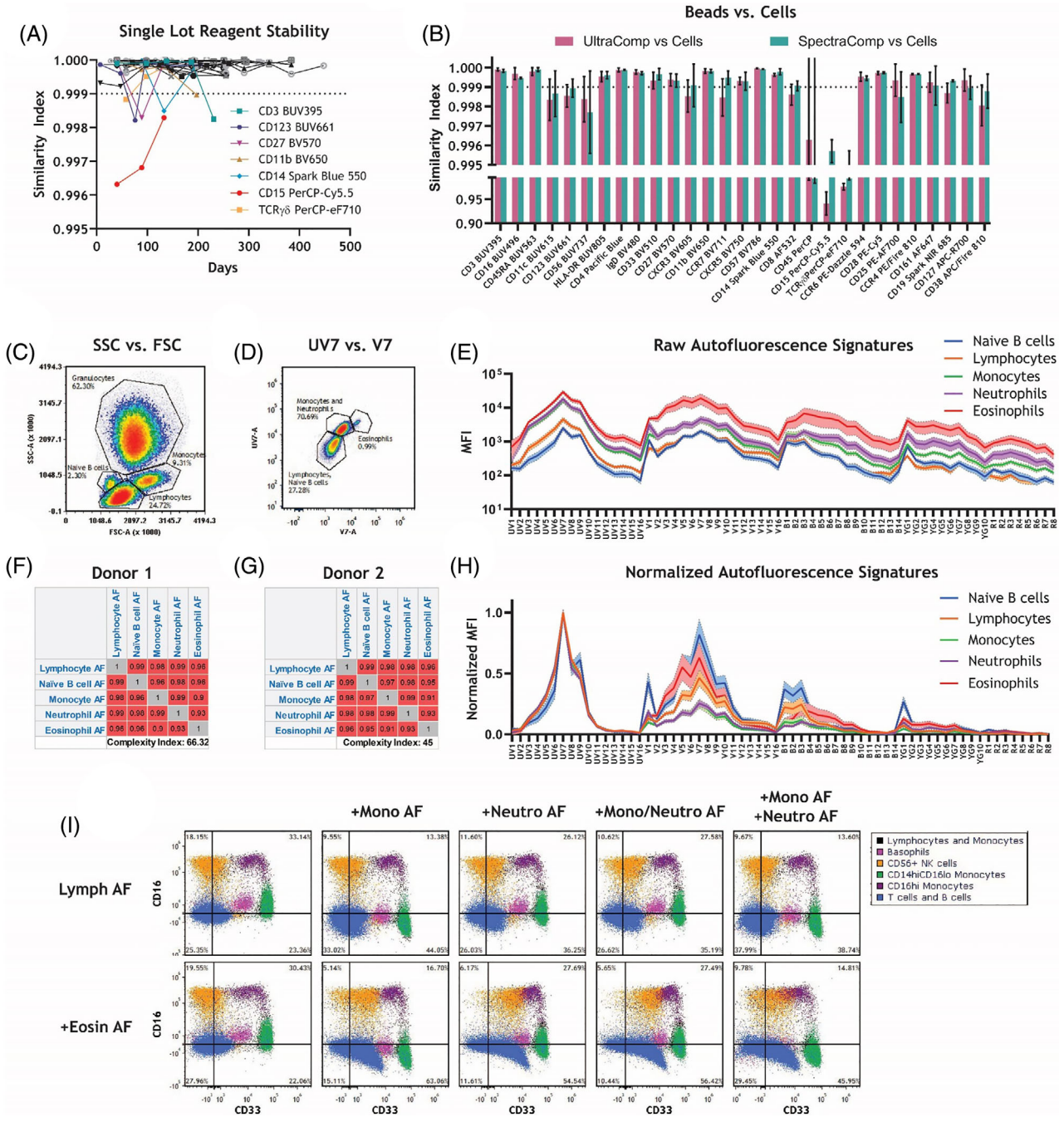

FIGURE 2 Interrogation of single-color reagent controls and autofluorescence unmixing. The Similarity Indices of successive reference control runs (intra-lot comparisons only) were captured over time (A). Most reagents (black and gray lines/dots) have Similarity Indices >0.9995 between multiple reference control capture points. Reagents that exhibit Similarity Indices <0.999 are highlighted with colored lines as shown: CD3 BUV395 (green line), CD123 BUV661 (purple), CD27 BV570 (pink), CD11b BV650 (brown), CD14 Spark Blue 550 (blue), CD15 PerCP-Cy5.5 (red), and TCRγδ PerCP-eF710 (orange). The spectral performances of each single antibody reagent on UltraComp and SpectraComp beads were compared to cells (B). Note that panel design was highly correlated to whether UltraComp, SpectraComp, or cells could be employed, as explored separately (Table 2). An example SSC versus FSC bivariate plot for one healthy blood donor is shown (C) next to a UV7 versus V7 raw data file plot (D). Populations with distinct UV7 versus V7 or SSC versus FSC characteristics are gated as shown and include lymphocytes, naïve B cells, monocytes, and granulocytes, which are subdivided into neutrophils and eosinophils. The raw autofluorescence signatures for these populations across 64 detectors on the Cytek Aurora are shown (E) for naïve B cells (blue), lymphocytes (orange), monocytes (green), neutrophils (purple), and eosinophils (red). Shaded envelopes indicate one standard deviation from the mean across 22 healthy donors. Similarity Index matrices for raw autofluorescence signatures are shown for two example donors in (F) and (G). The average normalized autofluorescence signatures of the same populations from (E) are shown in (H). The impact of different autofluorescence extraction setups on CD16 BUV496 and CD33 BV510 were compared (*I*). Using lymphocyte extraction (the lowest autofluorescence signature, top row) as default background, additional signatures for monocytes (+Mono AF), neutrophils (+Neutro AF), combined monocytes and neutrophils (+Mono/Neutro), or separate monocytes and neutrophils (+Mono AF + Neutro AF) with or without an additional eosinophil signature (+Eosin, bottom row) were extracted. The resulting CD16 BUV496 versus CD33 BV510 bivariate plots display colored overlays for T cells and B cells (blue), NK cells (orange), CD14hiCD16lo monocytes (green), CD16hi monocytes (purple) and basophils (pink). Quadrant centers are placed at origin for ease of comparison.

and HLA-DR BUV805 SpectraComp beads better recapitulated CD38 APC/Fire 810 staining on cells, with minor skewing of CD57 BV785 (Supplemental Figure 6).

For more deviant bead versus cell spectral profiles (or strong correlates thereof), optimal reference control format could vary. Spectrally correlated reagents CD57 BV785 and CD38 APC/Fire 810 could negatively impact one another, and UltraComp beads worked best for these two reagents to reduce unmixing errors in the HLA-DR BUV805 or CD57 BV785 channels (Supplemental Figure 6). Two other far red-emitting reagents, CD56 BUV737 and CD11b BV650, also benefitted from UltraComp beads to reduce unmixing errors. For the most unstable reagents CD123 BUV661 and CD15 PerCP-Cy5.5, freshly acquired cells remained preferable. Interestingly, TCRγδ PerCP-eF710 also exhibited poor similarity on both bead formats compared to cells, but employing SpectraComp beads improved TCRγδ resolution and eliminated false PerCP-Cy5.5 positivity on TCRγδ cells without negatively impacting CD127 APC-R700 (Supplemental Figure 6). This same improvement could be achieved using a CD4 surrogate for PerCP-eF710 on cells, which interestingly matched the SpectraComp-based but not the cell-based profile of TCRγδ PerCP-eF710 (Table 2, Supplemental Figure 7B).

To summarize, Similarity Index between either bead format and cells was not wholly predictive or representative of minute spectral profile differences that could have significant far-reaching impact. Reagents with high bead versus cell Similarity Indices and little-to-no discernable spectral differences (e.g., CD45RA BUV563 and CD14 Spark Blue 550) drove unmixing improvements when SpectraComp-based controls were applied. Meanwhile, no improvement was seen between reference control formats whose Similarity Indices matched less, for example, CD11c BUV615. And SpectraComp beads performed less well than UltraComp for some far-red emitting fluorophores such as BV785 and APC/Fire 810. In short, while this reference control optimization exercise revealed some fluorophore-specific features, panel design was highly correlated to whether UltraComp, SpectraComp or cells could be employed (Table 2).

3.4 | Autofluorescence

Current practice for spectral cytometry recommends applying the lowest autofluorescence (AF) signature available as unstained background, while incorporating brighter AF signatures as additional markers/colors. AF primarily impacts fluorophores with overlapping emission maxima in the UV4-UV10, the V4–V8 and less so the B1–B4 detectors on the Cytek Aurora. Due to the similarity in spectral profile between AF signatures and dim fluorophores like BUV496 and BV510 (Supplemental Figure 5B), AF signal may be interpreted as additional fluorophore signal during unmixing, leading to higher background and lower stain indices. This and other AF-induced phenomena were recently described in further detail [12].

We compared the AF signatures of populations identifiable on SSC versus FSC (Figure 2C) and UV7 versus V7 (Figure 2D) bivariate plots. UV7 versus V7 plots revealed three dominant AF signatures in non-fixed, RBC-lysed healthy donor whole blood: a low-AF lymphocyte signature, a high-AF monocyte/granulocyte signature, and a separate bright-AF eosinophil signature. These signatures were identifiable in 22 distinct healthy blood donors (Supplemental Figure 8A) and comparable signatures were identified in PBMC [12]. These distinct, raw AF spectral profiles show a successive increase in brightness from lymphocytes to monocytes, granulocytes, and eosinophils (Figure 2E). Interestingly, the Similarity Indices between intra-donor AF signatures could vary, but typically two pairs of populations always have high similarity: lymphocytes/naïve B cells and monocytes/neutrophils (Figure 2F,G). Normalized AF signatures (Figure 2H) can visually skew low-brightness populations to exhibit higher normalized signal in the V4–V8 region (Figure 2H).

We interrogated 10 distinct AF unmixing conditions using a lymphocyte gate as the lowest background, and then extracted either an additional monocyte signature, granulocyte signature, combined monocyte/granulocyte signature, or separate monocyte and granulocyte signatures, all with or without an additional eosinophil signature (Figure 2I). In general, extraction of an additional monocyte signature either alone or in combination with a granulocyte signature reduced the background of CD16 BUV496. However, CD16 BUV496 unmixing and CD33 BV510 resolution were negatively impacted by extraction of a high AF eosinophil signature. Moving forward, we selected a combined monocyte/neutrophil AF signature for extraction in addition to lymphocyte background.

3.5 | iCore precision and stability

We processed whole blood from three healthy donors and stained in triplicate at 0, 24, and 48 h post collection to assess iCore panel performance. Per-donor intra-assay precision (%CV) was determined at each timepoint across replicates for the 80+ distinct population gates (Figure 3). On average, we found that >95% of these distinct populations exhibit <20% CV at all queried timepoints, with lower cell counts trending toward higher %CV (Figure 4A–C). Immune subsets with lower cell counts that achieved <20 %CV include naïve (CD45RA+) and memory (CD45RA-) Tregs, follicular helper T cells (CD4+CXCR3-CXCR5+), nonswitched memory B cells (CD27+ IgD+), CD56hiCD16lo NK cells, CD11cloCD123hi pDCs, ILCs (Lin-CD127-), and CD15+CD16+ low-density granulocytes (LDGs). For some donors, myeloid-derived suppressor cell populations (M-MDSCs, PMN-MDSCs, and e-MDSCs) also passed precision. Interestingly, this suggests the iCore assay with fully optimized controls on the 5-laser Cytek Aurora system is more robust than a smaller, previously developed immune monitoring assay on the 4-laser system [13].

Additionally, the stability of immune populations on healthy donor blood collected in Na-Heparin tubes was assessed. As found previously [13], T cell polarization subsets (particularly those impacted by CXCR3), LDGs and pDCs were among the top altered immune subsets in peripheral blood processed 24 h post collection when using a student's t-test across inter-donor replicates (Figure 4E). Additional subsets distinguished by the iCore, such as T cell and B cell memory

TABLE 2 Reference control optimization

Marker	Fluorophore	Reference control	Comparision of cells, UltraComp beads, and SpectraComp beads for iCore reference controls
CD3	BUV395	SpectraComp	Interchangeable.
Viability	Live/Dead BLUE	Cells	-
CD16	BUV496	SpectraComp	Interchangeable. UltraComp beads improve BUV510. SpectraComp beads improve BUV395.
CD45RA	BUV563	SpectraComp	SpectraComp beads improve L/D, BUV496, BV570, AF532 and PE-Dazzle 594 compared to UltraComp beads. SpectraComp beads reduce background in BUV496 compared to cells.
CD11c	BUV615	SpectraComp	Interchangeable.
CD123	BUV661	Cells	Cells improve AF647 and Spark NIR 685 compared to either bead format.
CD56	BUV737	UltraComp	UltraComp beads improve BV750 and BV785 compared to SpectraComp beads or cells.
HLA-DR	BUV805	SpectraComp	SpectraComp beads improve APC/Fire 810 compared to UltraComp beads. SpectraComp beads can skew BV785.
CD4	Pacific Blue	SpectraComp	Interchangeable.
IgD	BV480	SpectraComp	Interchangeable.
CD33	BV510	SpectraComp	Interchangeable. Cells slightly reduce resolution of all markers,
CD27	BV570	SpectraComp	Interchangeable.
CXCR3	BV605	SpectraComp	Interchangeable.
CD11b	BV650	UltraComp	UltraComp beads improve BUV661, PE-Cy5, AF647 and Spark NIR 685 compared to SpectraComp beads or cells.
CCR7	BV711	SpectraComp	Interchangeable.
CXCR5	BV750	SpectraComp	Interchangeable.
CD57	BV786	UltraComp	UltraComp beads improve BV510 and APC/Fire 810 compared to SpectraComp beads or cells. SpectraComp beads can skew BUV805.
CD14	Spark Blue 550	SpectraComp	SpectraComp beads improve AF532 compared to UltraComp beads. Cells increase BUV469 background compared to SpectraComp beads.
CD8	AF532	SpectraComp	Interchangeable.
CD45	PerCP	SpectraComp	SpectraComp beads improve BUV661 compared to UltraComp beads or cells.
CD15	PerCP-Cy5.5	Cells	Cells improve AF647, Spark NIR 685 and APC-R700 compared to either bead format.
TCRγδ	PerCP-eF710	SpectraComp	SpectraComp beads improve PerCP-eF710 compared to UltraComp beads or cells. SpectraComp beads recapitulate cell-based CD4 PerCP-eF710 more so than TCRγδ on cells.
CCR6	PE-Dazzle 594	SpectraComp	Interchangeable.
CD28	PE-Cy5	SpectraComp	Interchangeable.
CD25	PE-AF700	SpectraComp	Interchangeable.
CCR4	PE/Fire 810	SpectraComp	Interchangeable.
CD161	AF647	SpectraComp	Interchangeable.
CD19	Spark NIR 685	SpectraComp	SpectraComp beads improve AF647 and APC-R700 compared to UltraComp beads.
CD127	APC-R700	SpectraComp	Interchangeable.
CD38	APC/Fire 810	UltraComp	UltraComp beads improve BV785 compared to SpectraComp beads or cells.

Note: The utility of UltraComp beads, SpectraComp beads, or cells as single stain controls was interrogated. N × N plots were used to survey unmixing results after 1 by 1 replacement with the different single stain formats per reagent. Example N × N plots supporting this table can be found in Supplemental Figure 6.

FIGURE 3 iCore gating scheme. A suggested gating strategy for the iCore is shown. The surveyed literature (Supplemental Figure 1K) was referenced to establish the current hierarchy which covers over 80 gates/populations. Additional gates or populations are possible but are not shown for simplicity. A comprehensive list of the gates can be found in Supplemental Table 1, and suggested fluor-minus-mulitple (FMM) controls are detailed in Supplemental Figure 11.

subsets (using CD27, CD28, and/or IgD), also displayed changes after 24 h. Statistically significant changes were either augmented at 48 h (Figure 4F) or show an opposite trend (i.e., a reduction after an increase at 24 h). Of note, very small shifts in %FoP can result in statistical significance due to highly precise values. However, intra-donor inter-timepoint %CVs revealed that only 16–21 populations out of

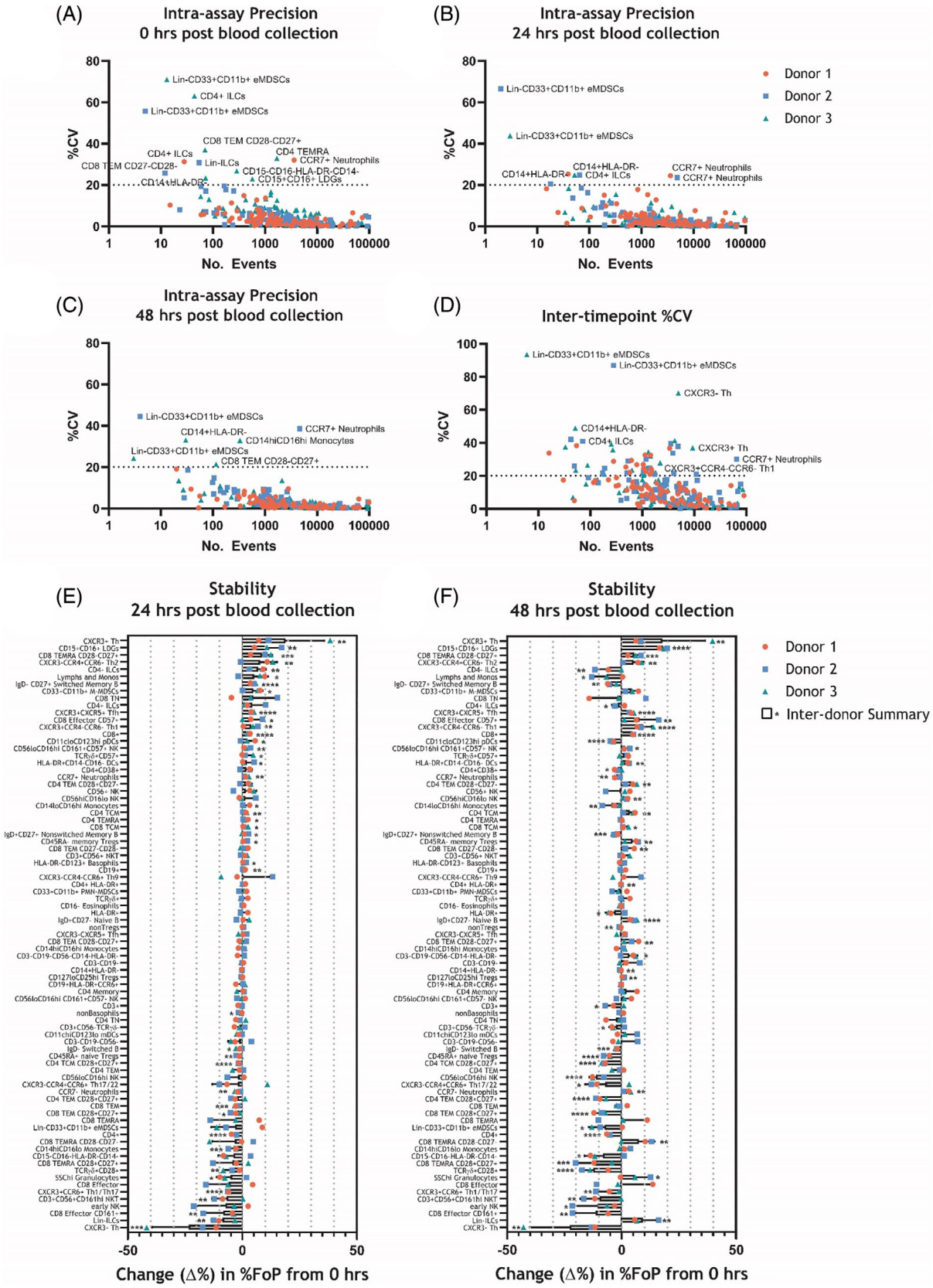

FIGURE 4 Legend on next page.

83 (about 22% of all gated immune subsets) failed stability based on 20% CV cutoff criteria (Figure 4D). These populations encompassed those with the highest %FoP changes previously mentioned (CXCR3+/CXCR3- and CD28/CD27 T cell subsets, pDCs, etc) as well as populations with very low cell counts (HLA-DR- populations, ILCs, etc).

3.6 | Biomarker drop-in application

The iCore offers six drop-in channels for customization: BV421, AF488 (or spectral equivalent FITC), PE, PE-Cy7, APC, and APC-Cy7 (or equivalent such as APC/Fire-750). The 36 normalized spectral profiles for the combined iCoreDrop can provide visual guidance on biomarker assignment (Figure 1). We regenerated the iCore CSI matrix with either CD4 or HLA-DR in each of the six drop-in channels to assess the impact by/on T cell or myeloid markers (Supplemental Figure 10). PE had the most impact on the iCore as CD4 (lymphoid marker), while PE-Cy7 and APC had a stronger impact when assigned HLA-DR (monocyte marker). Interestingly, the CD33 channel was much more broadly impacted during either drop-in condition, regardless of AF extraction method. However, these calculations showed that the drop-in positions are robust to the addition of abundant markers. We then selected six markers of interest for each of the drop-in modules and assigned the markers to open channels based on clone availability and minimally received spillover. For the T cell module, we selected CTLA-4 BV421, CD103 AF488, PD-1 PE, TIGIT PE-Cy7, CCR5 APC, and CD95 APC-Cy7 (Figure 5A). For the myeloid/B cell module, we selected CD117 BV421, CD163 AF488, CD141 PE, CD1c PE-Cy7, CD86 APC, and CD24 APC-Cy7 (Figure 5B). All drop-in reagents were titrated (Supplemental Figure 12) and subjected to general reference control checks.

The iCore performed similarly in the presence of drop-in markers, achieving highly identical %FoPs (Figure 5C,D) for all gated populations on two donors, except for certain rare-event populations such as MDSCs. This was mainly due to decreased resolution for CD33 BV510, which occurred for the iCoreDrop regardless of drop-in module, suggesting CD33 gating may require adjustments compared to that for the iCore. %CVs remained low; however, additional T cell markers increased the %CV of some T cell subsets including T(CM) and T(EM) for both CD4 and CD8s, and some CD28+CD27+ gated subsets. For the myeloid/B cell module, %CVs increased for some rare myeloid populations (e.g., CD14+HLA-DR-). To review the repeatability of the new drop-in channels, we developed example gating strategies to capture populations defined by the additional markers (Figure 5E,F). The queried gated populations have <20% CV across replicates, including for some very rare subsets in unstimulated samples (CD8+CD103+, CD4+CTLA-4+). Only CD141+ DCs have >20% CV (albeit <30% CV). Thus, we showed that the performance of the combined iCoreDrop was maintained and the drop-in channels were robust. We recommend the user perform further optimization for their specific needs when applying their own drop-in reagents. For example, we found that removing extraction of the additional monocyte/granulocyte AF signature could potentially improve the resolution of the AF488 and PE drop-in channels. Titration of drop-in reagents in the context of other iCore reagents, such as CD14 Spark Blue 550, could also allow improvement.

4 | DISCUSSION

There are increasing benefits to 30+ parameter flow cytometry. For example, identification of peripheral immune correlates to checkpoint inhibitor response has been successful in the context of higher-dimensional profiling [14, 15]. To date, several high-parameter spectral cytometry assays have been developed, but these 30+ spectral cytometry designs have not addressed the need for a drop-in strategy to enable user-specific biomarker interrogation.

The Standard BioTools MaxPar Direct Immune Profiling Kit for mass cytometry allows users to incorporate an additional seven markers if desired. We separately surveyed the literature and ultimately selected 29 iCore markers that are highly aligned with the MaxPar Direct Immune Kit, rendering our iCoreDrop immune monitoring assay a cost-effective equivalent for spectral cytometry. The six drop-in channels use bright and commonly available fluorophores, and application of the drop-in channels was highly robust in that (1) resolution and repeatability of the iCore populations were maintained and (2) drop-in reagents targeting low abundance or rare populations also exhibited high intra-assay precision. Additionally, open channels could be used for more creative workflows. The open PE channel, for example, could be utilized in the context of Infinity Flow, a recent Bioconductor package that enables interrogation of 100+ biomarkers across a backbone lineage panel [16].

While iterative marker-fluor reassignment was important to successful panel design (Supplemental Figure 9), resolution or background concerns were also addressed through staining or unmixing optimization. Interestingly, differences in bead versus cell spectral profiles and spectral profile stabilities appeared to be fluorophore-dependent, not marker dependent (i.e., the same concerns were noted for CD161 BUV661 and CD123 BUV661). This suggests that detailed

FIGURE 4 iCore precision and stability. The intra-assay precision (%coefficient of variation, or %CV) for the iCore was determined for three healthy blood donors at 0 h (A), 24 h (B), and 48 h (C) post blood collection. The %CV of three replicate samples is graphed against the average number of events across those replicates for Donor 1 (red dots), Donor 2 (blue squares), and Donor 3 (green triangles). Most populations (as gated in Figure 3) exhibit robust %CV <20% (dashed black line). Inter-operator and inter-instrument precision were not assessable at time of publication. Populations that have >20% for inter-timepoint precision either (1) fail intra-assay precision or (2) are statistically significantly different across timepoints (D). Only a few such populations are labeled for clarity. The average change in %Frequency of Parent population (% FoP) per donor from baseline analysis at 0 h was determined at 24 h (E) and 48 h (F). Populations are ordered from greatest average inter-donor increase to greatest inter-donor decrease. White bars indicate the average change across donors with inter-donor error shown. A student's t-test was applied to assess the significance of the %FoP change across the donors, which for each population are indicated with * (p <0.05), ** (p <0.01), *** (p <0.001), or **** (p <0.0001). Some populations are statistically significantly different despite otherwise minimal change in %FoP. Corresponding data values for this figure are tabulated in Supplemental Table 1.

(A)

T cell Drop-In Reagents

Marker	Clone	Fluorophore	Vendor	Catalog No.	Stock Conc. (µg/ml)	µl per test	Staining
CTLA-4	BNI3	BV421	Biolegend	369605	100	1.25	4C, 45 min
CD103	Ber-ACT8	AF488	Biolegend	350208	100	0.31	4C, 45 min
PD-1	EH12.2H7	PE	Biolegend	329905	50	1.25	4C, 45 min
TIGIT	MBSA43	PE-Cy7	Thermo	25-9500-41	50	2.50	4C, 45 min
CCR5	2D7/CCR5	APC	BD	561748	50	5.00	4C, 45 min
CD95	DX2	APC-Cy7	Biolegend	305635	200	0.31	4C, 45 min

(B)

Myeloid/B cell Drop-In Reagents

Marker	Clone	Fluorophore	Vendor	Catalog No.	Stock Conc. (µg/ml)	µl per test	Staining
CD117	104D2	BV421	Biolegend	313215	50	0.63	4C, 45 min
CD163	MAC2-158	AF488	Thermo	53-1637-41	25	2.50	4C, 45 min
CD141	AD5-14H12	PE	Miltenyi	130-113-880	50	2.50	4C, 45 min
CD1c	L161	PE-Cy7	Biolegend	331515	100	0.31	4C, 45 min
CD86	IT2.2	APC	Biolegend	305411	200	0.31	4C, 45 min
CD24	ML5	APC-Cy7	Biolegend	311131	300	0.63	4C, 45 min

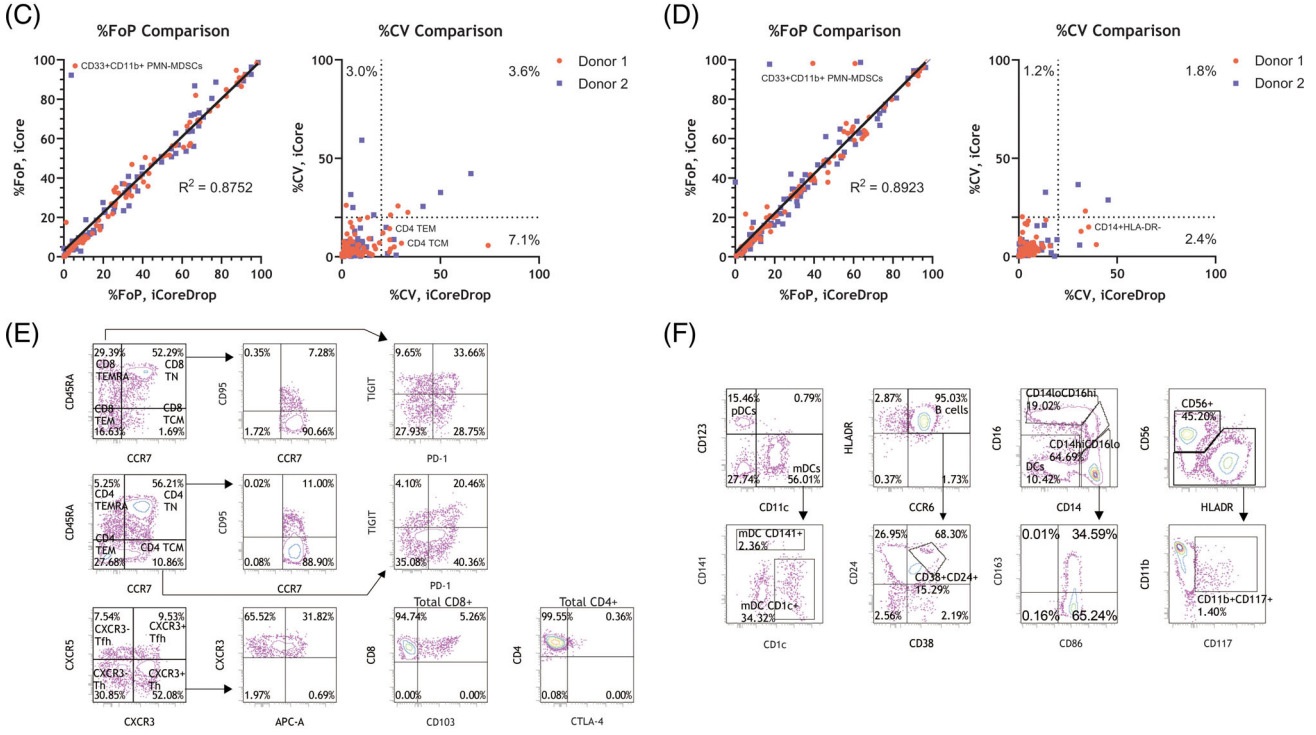

(G)

Population	Donor 1 Average %FoP	Donor 1 %CV	Donor 2 Average %FoP	Donor 2 %CV
CD8+CD45RA+CCR7+CD95+T(SCM)	7.95	10.18	6.69	13.12
CD4+CD45RA+CCR7+CD95+T(SCM)	11.47	5.91	11.8	1.82
CXCR3+Th CCR5+	59.59	4.79	55.44	3.73
CD8 Effector PD-1+TIGIT+	34.29	2.35	28.2	6.99
CD4 Memory PD-1+TIGIT+	19.97	5.15	23.02	9.18
CD8+CD103+	4.43	8.19	2.6	11.56
CD4+CTLA-4+	0.28	26.49	0.56	16.98

(H)

Population	Donor 1 Average %FoP	Donor 1 %CV	Donor 2 Average %FoP	Donor 2 %CV
CD11chiCD123lo CD1c+(cDC2-3)	35.57	1.28	65.63	1.07
CD11chiCD123lo CD141+(cDC1)	1.99	16.79	3.12	28.72
CD14hiCD16lo CD86+CD163-	63.84	2.00	66.69	0.36
CD14hiCD16lo CD86+CD163+	36.01	3.50	31.19	2.42
CD38+CD24+Transitional B cells	13.72	2.81	18.49	2.46
CD11b+CD117+Myeloblasts	1.42	1.86	1.27	12.84

FIGURE 5 Drop-in application. A T cell drop-in module (A) and myeloid/B cell drop-in module (B) were tested using the reagents assigned to open channels BV421, AF488, PE, PE-Cy7, APC, and APC-Cy7 as shown. Reagents were first titrated (Supplemental Figure 12). The %FoP and % CV of replicate gated populations were compared between the iCore with and without the presence of drop-in markers for the T cell module (C) or myeloid/B cell module (D). Populations representative of %FoP or %CV changes are labeled. Gating strategies defined by the additional markers were developed (E, F) to assess drop-in channel precision. The resulting %FoP and intra-assay %CV for the new populations are tabulated for the T cell (G) and myeloid/B cell (H) gating.

characterization of intrinsic fluorophore behavior may be beneficial for eliminating additional controls and troubleshooting unmixing errors. While the Cross Stain Index matrix or other spillover spreading matrix provides useful information toward conventional impacting/impacted fluorophore pairs, the Similarity Index matrix may provide additional insight into panel design in the context of spectral cytometry. Spectrally correlated fluorophores (i.e., those with higher Similarity Indices) are mutually impactful, and single stain control optimization greatly improved spectrally correlated markers compared to neighboring or tandem-related fluorophores.

That said, Similarity Index can fail to predict whether small differences in spectral profiles have significant and far-reaching effects. For example, CD11c BUV615 had a lower Similarity Index between both bead formats and cells, but these formats are interchangeable during

unmixing. For CD45RA BUV563, Similarity Indices were highly identical between UltraComp beads, SpectraComp beads and cells, but each format performed differently. TCRγδ PerCP-eF710 on cells has no spectrally equivalent replacement, but despite the lower Similarity Indices between beads and cells, SpectraComp beads improved TCRγδ resolution and prevented unmixing errors. We did note that reagents with far-red emitting fluorophores (CD56 BUV737, CD11b BV650, CD57 BV785, CD38 APC/Fire 810) tended to perform better on UltraComp beads. In short, any generalizations regarding interchangeability of cells and bead formats are precluded by the panel design itself, which dictates whether small spectral deviations will affect the resolution of marker-fluorophores that have correlated local emission maxima.

The application of spectral cytometry in the clinical space is an exciting prospect, and guidance on cross-instrument standardization has been reported [8]. Additionally, the Cytek SpectroFlo reference library is an auxiliary feature that enables large assay deployment sans expensive daily controls. Establishment of best practices for the reference library is ongoing. Reference controls stored once a month may be suitable for most reagents, but not all, considering some fluorophores may exhibit changes week to week. Surrogate reference controls (e.g., CD4-based) may deviate from panel reagents, and different background formats (such as bead vs. cells or PBMC vs. blood) may provide high SIs >0.999 but nonetheless cause far-reaching negative impact. Clarity in understanding what single stain controls can and cannot be used, and the associated timeframe for recapture, is needed to reduce ambiguous unmixing errors and prevent time-consuming troubleshooting tasks.

A remaining challenge to reagent and reference control tracking is day-to-day feasibility. SpectroFlo offers in-software calculation of Similarity Index, but methods to extract or revisit the Similarity Indices of stored reference controls are not intuitive, requiring either screenshot capture or export and external calculation. Ideally, comparison of experiment controls to benchmarks would be reviewed before unmixing, but currently multiple unmixing windows must be advanced before this step. An option to select entire reference control sets to prevent tedious click-through tasks would be highly beneficial. Lastly, exploration of autofluorescence signatures is a highly manual process; other spectral cytometry applications employ an AF Finder tool to facilitate this [17]. In the future, we hope to see advanced clinical-enabling features within all cytometry software to empower the evolving requirements for high-precision spectral cytometry.

5 | CONCLUSION

We developed a pan-immune monitoring spectral cytometry assay on the Cytek Aurora for cross-program applications, while opting for six additional drop-in channels such that biomarkers of interest could be incorporated. The 30-color iCore (29 immune markers plus viability) exhibits high intra-assay precision that was maintained in the presence of additional drop-in markers, and the drop-in channels themselves were highly robust. Extensive interrogation of the single stain reagents, reference control formats and autofluorescence extraction was necessary to achieve this result, and we emphasize that optimized reference control practices are an absolute requirement for successful application of spectral cytometry assays.

ACKNOWLEDGMENTS

Thanks to the onsite Volunteer Donation Program at BMS in Redwood City, CA for providing healthy human blood samples.

CONFLICT OF INTEREST

The authors have no conflicts of interest to declare.

PEER REVIEW

The peer review history for this article is available at https://publons.com/publon/10.1002/cyto.a.24708.

REFERENCES

1. Park LM, Lannigan J, Jaimes MC. OMIP-069: forty-color full spectrum flow cytometry panel for deep immunophenotyping of major cell subsets in human peripheral blood. Cytometry A. 2020;97(10):1044–51. https://doi.org/10.1002/cyto.a.24213
2. Sahir F, Mateo JM, Steinhoff M, Siveen KS. Development of a 43 color panel for the characterization of conventional and unconventional T-cell subsets, B cells, NK cells, monocytes, dendritic cells, and innate lymphoid cells using spectral flow cytometry. Cytometry A. 2020;1–7. https://doi.org/10.1002/cyto.a.24288
3. Wang SR, Zhong N, Zhang XM, Zhao ZB, Balderas R, Li L, et al. OMIP 071: a 31-parameter flow cytometry panel for In-depth Immunophenotyping of human T-cell subsets using surface markers. Cytometry A. 2021;99(3):273–7. https://doi.org/10.1002/cyto.a.24272
4. Asano T, Boisson B, Onodi F, Matuozzo D, Moncada-Velez M, Maglorius Renkilaraj MRL, et al. X-linked recessive TLR7 deficiency in ~1% of men under 60 years old with life-threatening COVID-19. Sci Immunol. 2021;6(62). https://doi.org/10.1126/sciimmunol.abl4348
5. Nogimori T, Sugawara Y, Higashiguchi M, Murakami H, Akita H, Takahama S, et al. OMIP 078: a 31-parameter panel for comprehensive immunophenotyping of multiple immune cells in human peripheral blood mononuclear cells. Cytometry A. 2021;99(9):893–8. https://doi.org/10.1002/cyto.a.24490
6. Fernandez MA, Alzayat H, Jaimes MC, Kharraz Y, Requena G, Mendez P. High-dimensional Immunophenotyping with 37-color panel using full-Spectrum cytometry. Methods Mol Biol. 2022;2386:43–60. https://doi.org/10.1007/978-1-0716-1771-7_4
7. Bagwell CB, Hunsberger B, Hill B, Herbert D, Bray C, Selvanantham T, et al. Multi-site reproducibility of a human immunophenotyping assay in whole blood and peripheral blood mononuclear cells preparations using CyTOF technology coupled with Maxpar Pathsetter, an automated data analysis system. Cytometry B Clin Cytom. 2020;98(2):146–60.
8. McCausland M, Lin Y, Nevers T, Groves C, Decman V. With great power comes great responsibility: high-dimensional spectral flow cytometry to support clinical trials. Bioanalysis. 2021;13(21):1597–616. https://doi.org/10.4155/bio-2021-0201
9. Ferrer-Font L, Small SJ, Lewer B, Pilkington KR, Johnston LK, Park LM, et al. Panel optimization for high-dimensional Immunophenotyping assays using full-Spectrum flow cytometry. Curr Protoc. 2021;1(9):e222. https://doi.org/10.1002/cpz1.222
10. Bonilla DL, Reinin G, Chua E. Full Spectrum flow cytometry as a powerful Technology for Cancer Immunotherapy Research. Front Mol Biosci. 2021;7:612801. https://doi.org/10.3389/fmolb.2020.612801
11. Phitonex Inc. Above + beyond 40 colors [White paper]. Phitonex; 2020.

12. Jameson VJ, Luke T, Yan Y, Hind A, Evrard M, Man K, et al. Unlocking autofluorescence in the era of full spectrum analysis: implications for immunophenotype discovery projects. Cytometry A. 2022;101:922–41. https://doi.org/10.1002/cyto.a.24555
13. Jensen HA, Wnek R. Analytical performance of a 25-marker spectral cytometry immune monitoring assay in peripheral blood. Cytometry A. 2020;99(2):180–93. https://doi.org/10.1002/cyto.a.24290
14. Krieg C, Nowicka M, Guglietta S, Schindler S, Hartmann FJ, Weber LM, et al. High-dimensional single-cell analysis predicts response to anti-PD-1 immunotherapy. Nat Med. 2018;24:144–53. https://doi.org/10.1038/nm.4466
15. Woods D, Laino AS, Winters A, Alexandre J, Freeman D, Rao V, et al. Nivolumab and ipilimumab are associated with distinct immune landscape changes and response-associated immunophenotypes. JCI Insight. 2020;5:e137066. https://doi.org/10.1172/jci.insight.137066
16. Becht E, Tolstrup D, Dutertre C, Morawski PA, Campbell DJ, Ginhoux F, et al. High-throughput single-cell quantification of hundreds of proteins using conventional flow cytometry and machine learning. Sci Adv. 2021;7(39):eabg0505. https://doi.org/10.1126/sciadv.abg0505
17. Wanner N, Barnhart J, Apostolakis N, Zlojutro V, Asosingh K. Using the autofluorescence finder on the Sony ID7000™ spectral cell analyzer to identify and Unmix multiple highly autofluorescent murine Lung populations. Front Biogen Biotechnol. 2022;10. https://doi.org/10.3389/fbioe.2022.827987

SUPPORTING INFORMATION

Additional supporting information can be found online in the Supporting Information section at the end of this article.

How to cite this article: Jensen HA, Kim J. iCoreDrop: A robust immune monitoring spectral cytometry assay with six open channels for biomarker flexibility. Cytometry. 2022. https://doi.org/10.1002/cyto.a.24708